applied sciences

MDPI

Article

A Single-Stage LED Tube Lamp Driver with Power-Factor Corrections and Soft Switching for Energy-Saving Indoor Lighting Applications

Chun-An Cheng, En-Chih Chang *, Ching-Hsien Tseng and Tsung-Yuan Chung

Department of Electrical Engineering, I-Shou University, Dashu District, Kaohsiung City 84001, Taiwan; cacheng@isu.edu.tw (C.-A.C.); isu10101001m@cloud.isu.edu.tw (C.-H.T.); isu10001008m@cloud.isu.edu.tw (T.-Y.C.)

* Correspondence: enchihchang@isu.edu.tw; Tel.: +886-7-657-7711 (ext. 6642)

Academic Editor: Eric Ka-wai Cheng

Received: 4 November 2016; Accepted: 17 January 2017; Published: 24 January 2017

Abstract: This paper presents a single-stage alternating current (AC)/direct current (DC) light-emitting diode (LED) tube lamp driver for energy-saving indoor lighting applications; this driver features power-factor corrections and soft switching, and also integrates a dual buck-boost converter with coupled inductors and a half-bridge series resonant converter cascaded with a bridge rectifier into a single-stage power-conversion topology. The features of the presented driver are high efficiency (>91%), satisfying power factor (PF > 0.96), low input-current total-harmonic distortion (THD < 10%), low output voltage ripple factor (<7.5%), low output current ripple factor (<8%), and zero-voltage switching (ZVS) obtained on both power switches. Operational principles are described in detail, and experimental results obtained from an 18 W-rated LED tube lamp for T8/T10 fluorescent lamp replacements with input utility-line voltages ranging from 100 V to 120 V have demonstrated the functionality of the presented driver suitable for indoor lighting applications.

Keywords: converter; driver; light-emitting diode (LED)

1. Introduction

Latest developments and applications of solid-state lighting have begun gaining greater attention due to the requirements for efficient energy usage nowadays [1–16]. With features of energy-savings, lower maintenance costs and long lifetime, light-emitting diode (LED) tube lamps have begun to be favorable alternatives to replace traditional T8/T10-type fluorescent lamps in building-lighting applications [17–19]. According to the specifications shown in [20,21] with almost the same color temperature and color-rendering index, the LED tube lamp has better lighting efficiency, less power consumption, longer lamp lifetime, and contains no mercury inside the lamp tube, as compared to its T8-type counterparts. Therefore, T8-type LED tube lamps have become increasingly popular lighting sources for indoor lighting applications such as public architecture, offices, classrooms, and so on [17–21]. Figure 1 shows the commercial two-stage driver for supplying a T8-type LED tube lamp; it is composed of an AC-DC (alternating current-direct current) converter (typically a boost converter) with power-factor corrections (PFCs) as the first stage, and a DC-DC converter (typically a buck converter) as the second stage for regulating the voltage/current of the LED tube lamp. Separate controllers for each stage are required, and the circuit efficiency is restricted due to the two-stage power conversion. Some single-stage AC-DC drivers for providing a T8-type LED tube lamp to replace T8/T10-type fluorescent lamps have been presented: reference [18] utilizes a flyback PFC converter, and a buck converter with input-current shaping is presented in reference [19]. These single-stage versions are cost-effective in comparison to their two-stage counterpart; however, their power switches do not include the soft-switching function, which results in limited efficiency.

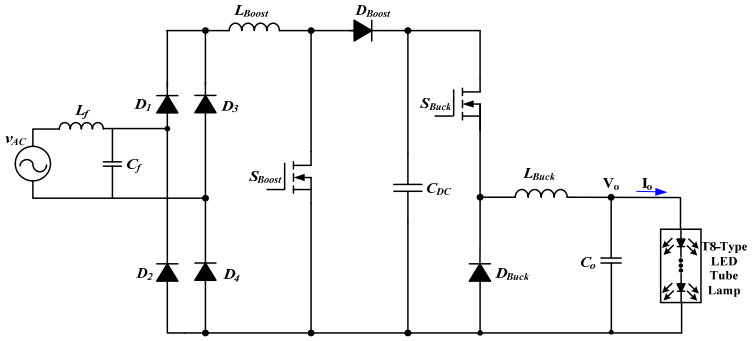

Figure 1. The commercial two-stage driver for supplying a T8-Type LED (light-emitting diode) tube lamp.

In response to these concerns, this paper presents a single-stage LED tube lamp driver suitable for indoor lighting applications with features of power-factor corrections and soft-switching characteristics. Theoretical analyses of operating modes, design equations for key circuit parameters, and experimental results from a prototype driver circuit for supplying an 18 W-rated T8-type LED tube lamp with input voltages ranging from 100 V to 120 V are demonstrated. This paper is organized as follows. Section 2 introduces and analyzes the presented single-stage LED tube lamp driver. Section 3 shows design equations of key components in the presented driver. Section 4 demonstrates experimental results of a prototype circuit for supplying an LED tube lamp. Finally, some conclusions are provided in Section 5.

2. The Description and Analysis of the Presented LED Tube Lamp Driver

Figure 2 shows the presented driver, which integrates the dual buck-boost converter with coupled inductors (one buck-boost converter includes a diode D_{b1}, a coupled inductor L_{PFC1}, a switch S_1, a body diode of the switch S_2, and a DC-linked capacitor C_{DC1}; another buck-boost converter includes a diode D_{b2}, a coupled inductor L_{PFC2}, a switch S_2, a body diode of the switch S_1, and the capacitor C_{DC2}) with the half-bridge series resonant converter cascaded with a bridge rectifier (including two DC-linked capacitors C_{DC1} and C_{DC2}, two switches S_1 and S_2, a resonant inductor L_r, a resonant capacitor C_r, a full-bridge rectifier (including diodes D_1, D_2, D_3 and D_4), and an output capacitor C_o) into a single-stage topology for supplying an LED tube lamp [17]. In addition, an LC filter (an inductor L_f and a capacitor C_f) is connected with the input utility-line voltage.

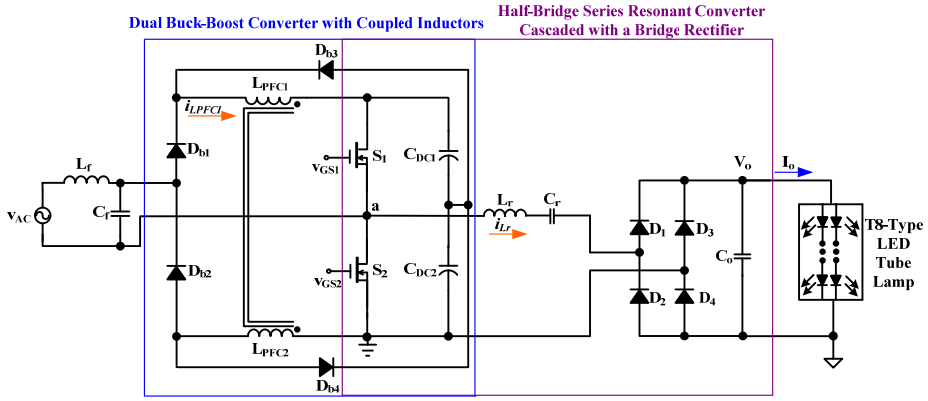

Figure 2. The presented single-stage driver for supplying a T8-type LED tube lamp.

In order to analyze the operations of the presented LED tube lamp driver, the following assumptions are made.

(a) Since the switching frequencies of the two switches (S_1 and S_2) are much higher than that of the utility-line voltage v_{AC}, the sinusoidal utility-line voltage can be considered as a constant value for each high-frequency switching period.
(b) Power switches are complementarily operated, and their intrinsic diodes and inherent drain-source capacitors are considered.
(c) The conducting voltage drops of all diodes (including D_{b1}, D_{b2}, D_{b3}, D_{b4}, D_1, D_2, D_3 and D_4) are neglected.
(d) Two coupled inductors (L_{PFC1} and L_{PFC2}) are designed to be operated in discontinuous-conduction mode (DCM) for naturally achieving power-factor correction (PFC).

The operating modes and key waveforms of the presented LED tube lamp driver during the positive half-cycle of input utility-line voltage are shown in Figures 3 and 4, respectively, and the analysis of operations for the presented driver are described in detail as follows.

Mode 1 ($t_0 \leq t < t_1$; in Figure 3a): The drain-source voltage v_{DS1} of S_1 is decreased to zero at time t_0; thus, the body diode of switch S_1 is forward-biased. The resonant capacitor C_r provides energy to resonant inductor L_r, capacitors C_{DC1}, C_{DC2}, C_o and the LED tube lamp through S_1's body diode, D_2, and D_3. When power switch S_1 turns on with zero-voltage switching (ZVS) at t_1, this mode ends.

Mode 2 ($t_1 \leq t < t_2$; in Figure 3b): This mode begins when switch S_1 achieves ZVS turn-on at t_1. The input voltage v_{AC} provides energy to coupled inductor L_{PFC1} through diode D_{b1} and switch S_1. The inductor current i_{LPFC1} linearly increases from zero, and can be expressed as

$$i_{LPFC1}(t) = \frac{\sqrt{2}v_{AC-rms}\sin(2\pi f_{AC}t)}{L_{PFC1}}(t - t_1). \tag{1}$$

where $v_{AC\text{-}rms}$ is the root-mean-square (rms) value of the input utility-line voltage, and f_{AC} is the utility-line frequency.

The resonant capacitor C_r still provides energy to inductor L_r, capacitors C_{DC1}, C_{DC2}, C_o and the LED tube lamp through S_1, D_2, and D_3. This mode finishes when the resonant inductor current i_{Lr} is zero at t_2.

Mode 3 ($t_2 \leq t < t_3$; in Figure 3c): The input voltage v_{AC} still provides energy to the coupled inductor L_{PFC1} through diode D_{b1} and switch S_1. The DC-bus capacitors C_{DC1} and C_{DC2} supply energy to resonant inductor L_r, capacitors C_r and C_o, and the LED tube lamp through switch S_1, D_1, and D_4. This mode ends when inductor current i_{LPFC1} reaches its peak value at t_3, which is denoted as $i_{LPFC1\text{-}pk}(t)$, and can be expressed as

$$i_{LPFC1-pk}(t) = \frac{\sqrt{2}v_{AC-rms}\sin(2\pi f_{AC}t)}{L_{PFC1}}DT_S. \tag{2}$$

where D and T_S are the duty cycle and period, respectively, of the power switch.

Mode 4 ($t_3 \leq t < t_4$; in Figure 3d): This mode begins when S_1 turns off at t_3. The utility-line voltage v_{AC} and the coupled inductor L_{PFC1} supply energy to the drain-source capacitor of S_1 through diode D_{b1}.

The DC-bus capacitors C_{DC1} and C_{DC2}, the drain-source capacitor of S_2 and resonant inductor L_r provide energy to capacitors C_r and C_o and the LED tube lamp through diodes D_1 and D_4. When the drain-source voltage v_{DS2} of S_2 is decreased to zero at t_4, this mode ends.

Mode 5 ($t_4 \leq t < t_5$; in Figure 3e): This mode begins when the body diode of switch S_2 is forward-biased at t_4. The coupled inductor L_{PFC1} provides energy to C_{DC1} through diode D_{b3}. The inductor current i_{LPFC1} linearly decreases, and can be given by

$$i_{LPFC1}(t) = \frac{\sqrt{2}v_{AC-rms}\sin(2\pi f_{AC}t) - V_{DC}/2}{L_{PFC1}}(t - t_4). \tag{3}$$

where $V_{DC}/2$ is the voltage of the DC-linked capacitor C_{DC1}.

Inductor L_r provides energy to capacitors C_r and C_o and the LED tube lamp through S_2's body diodes, D_1 and D_4. When power switch S_2 is turned on with ZVS at t_5, this mode ends.

Mode 6 ($t_5 \leq t < t_6$; in Figure 3f): This mode begins when switch S_2 achieves ZVS turn-on at t_5. Inductor L_r continues providing energy to capacitors C_r and C_o and the LED tube lamp through S_2, D_1 and D_4. The mode ends when the resonant inductor current i_{Lr} decreases to zero at t_6.

Mode 7 ($t_6 \leq t < t_7$; in Figure 3g): This mode begins when current i_{Lr} decreases to zero at t_6. Capacitor C_r provides energy to inductor L_r, capacitor C_o and the LED tube lamp through S_2 and diodes D_2 and D_3. The mode ends when switch S_2 turns off at t_7.

Mode 8 ($t_7 \leq t < t_8$; in Figure 3h): In this mode, capacitor C_r and the drain-source capacitor of switch S_1 provide energy to inductor L_r, the drain-source capacitor of S_2, capacitors C_{DC1}, C_{DC2}, C_o, and the LED tube lamp through diodes D_2 and D_3. When the drain-source voltage v_{DS1} of S_1 is decreased to zero at t_7, this mode ends. Then, *Mode 1* begins for the next high-frequency switching period.

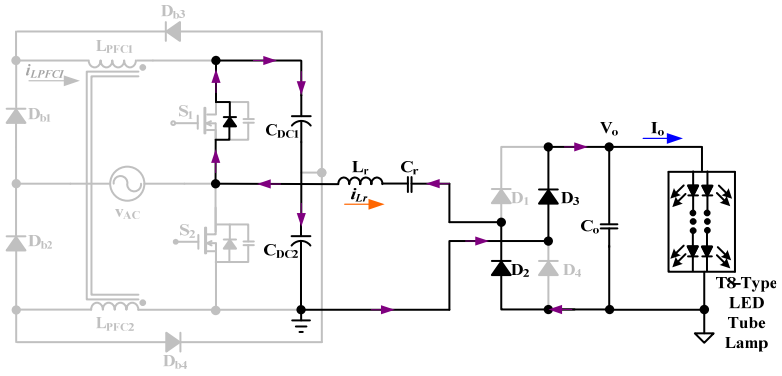

(**a**)

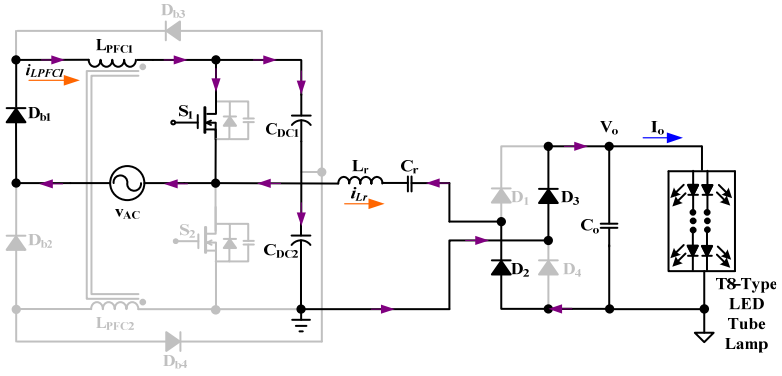

(**b**)

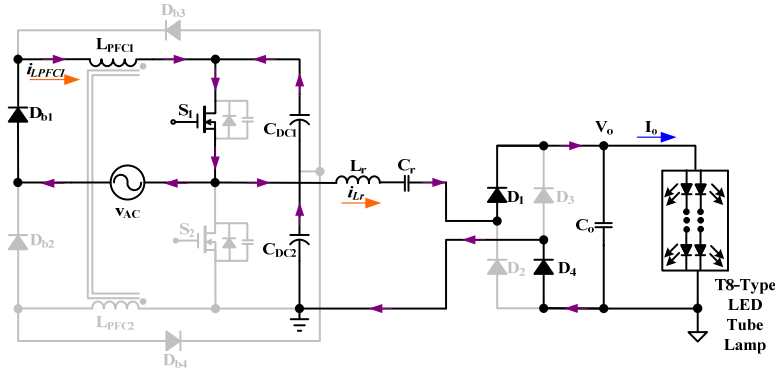

(**c**)

Figure 3. *Cont.*

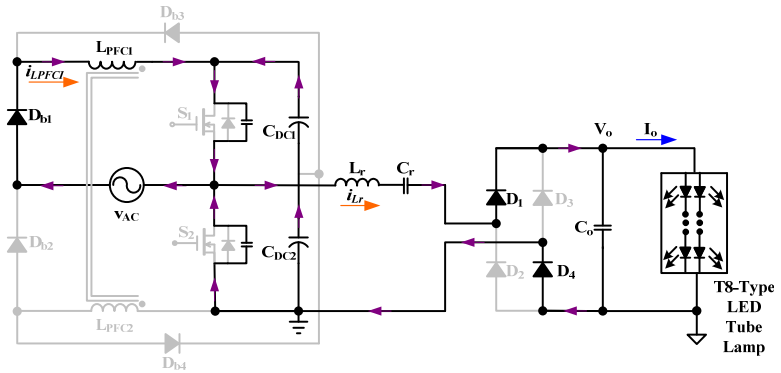

(**d**)

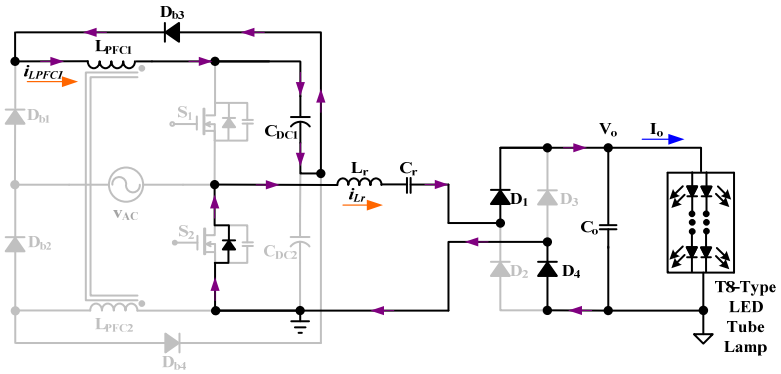

(**e**)

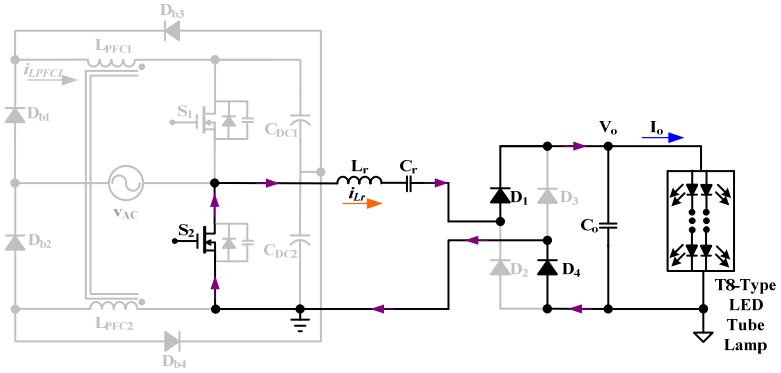

(**f**)

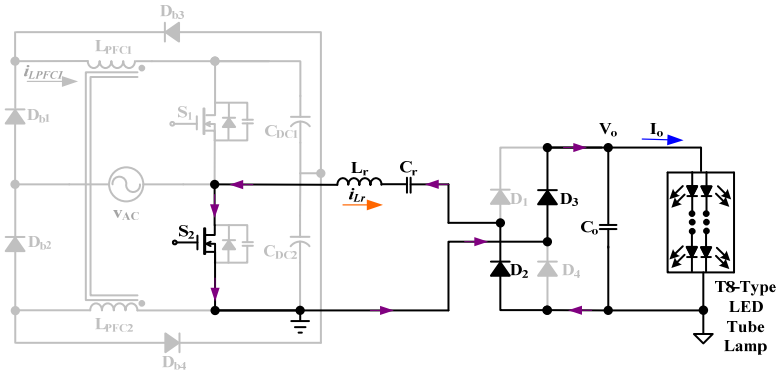

(**g**)

Figure 3. *Cont.*

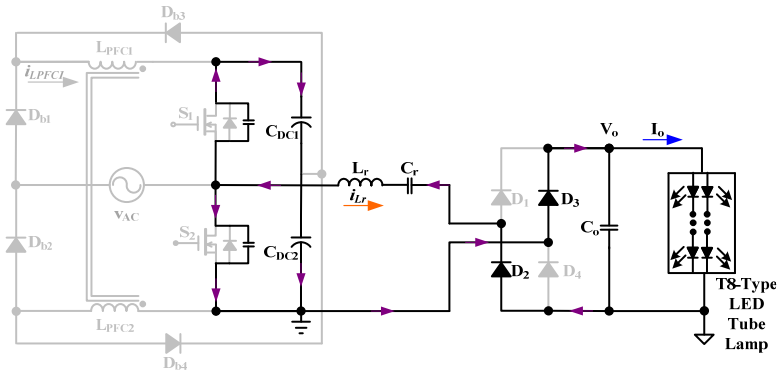

(**h**)

Figure 3. Operation modes of the presented driver during the positive half-cycle of input voltage v_{AC}. (**a**) *Mode* 1; (**b**) *Mode* 2; (**c**) *Mode* 3; (**d**) *Mode* 4; (**e**) *Mode* 5; (**f**) *Mode* 6; (**g**) *Mode* 7; (**h**) *Mode* 8.

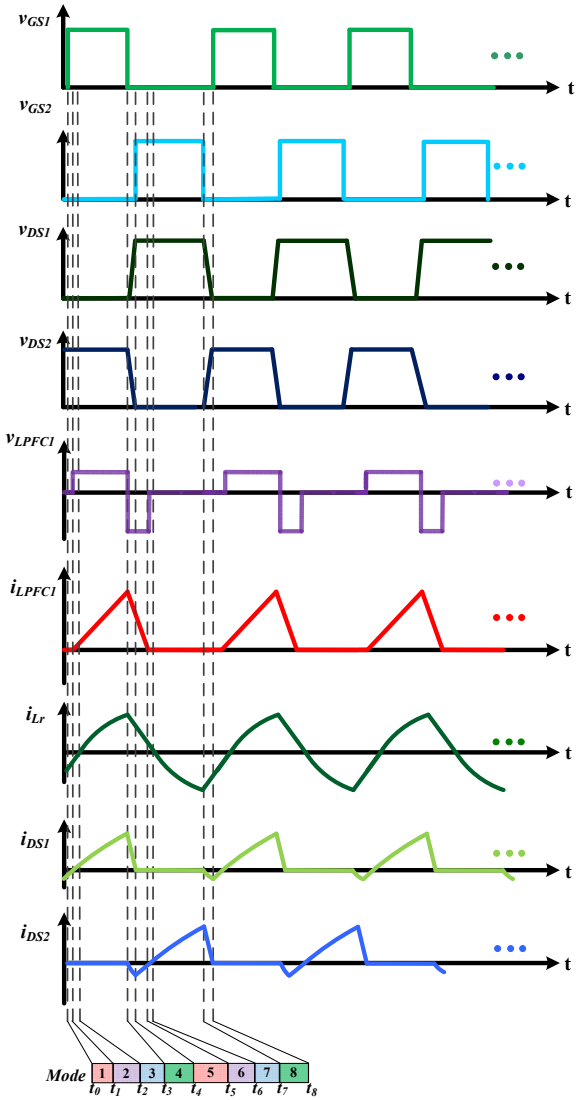

Figure 4. Key waveforms of the presented LED tube lamp driver during the positive half-cycle of the input utility-line voltage.

Figure 5 shows the circuit diagram for controlling the single-stage LED tube lamp driver. Referring to Figure 5 and utilizing a constant voltage/current controller (IC1 SEA05) for regulating the LED tube lamp's output voltage and current, the output voltage V_o can be sensed through resistors R_{vs1}, VR_1 and R_{vs2}, and the output current can be sensed through resistor R_3. The sensed output signal from pin 5 of the IC1 feeds into the high-voltage resonant controller (IC3 ST L6599) through a photo-coupler (IC2 PC817). Two gate-driving signals v_{GS1} and v_{GS2} are generated from pin 15 and pin 11, respectively, of the IC3, to carry out regulating the LED tube lamp's output voltage and current. In addition, an AC-DC switching power module with dual output voltages is utilized for providing the 15 V power supply voltages of IC1 and IC3 in the control circuit.

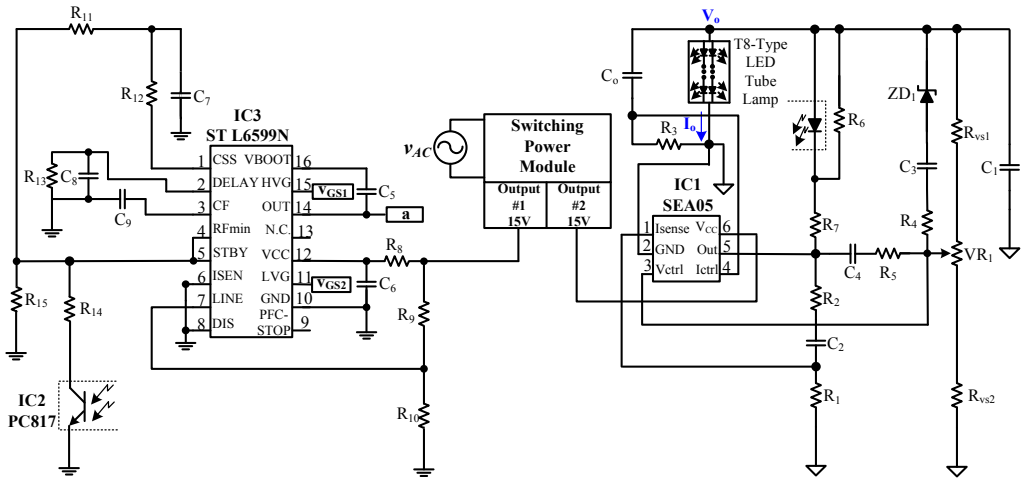

Figure 5. The utilized control circuit for the presented LED tube lamp driver.

3. Design Equations of Key Components in the Presented LED Tube Lamp Driver

3.1. Design of Coupled Inductors L_{PFC1} and L_{PFC2}

The design equation of the coupled inductor L_{PFC1} (L_{PFC2}) is expressed as [22]

$$L_{PFC1} = \frac{\eta {v_{AC-rms}}^2 D^2}{2P_{lamp} f_S} = L_{PFC2} \tag{4}$$

where η is the estimated circuit efficiency, P_{lamp} is the rated power of the LED tube lamp, and f_S is the switching frequency.

With a η of 0.9, a $v_{AC\text{-}rms}$ of 110 V and a P_{lamp} of 18 W, an f_S of 55 kHz and a D of 0.5, the coupled inductors L_{PFC1} and L_{PFC2} are given by:

$$L_{PFC1} = L_{PFC2} = \frac{0.9 \times 110^2 \times 0.5^2}{2 \times 18 \times 55,000} = 1.34 \text{ mH}.$$

3.2. Design of Series Resonant Tank L_r and C_r

Figure 6 depicts the equivalent circuit during the design of the series resonant tank; R_o is the equivalent resistance of the T8-type LED tube lamp, and can be represented by $R_o = V_o/I_o$. By using the fundamental approximation theory, the fundamental components of the switch voltage v_{DS2} can be expressed by [23,24]

$$v_{DS2-fund} = \frac{2}{\pi} V_{DC} \sin 2\pi f_S t. \tag{5}$$

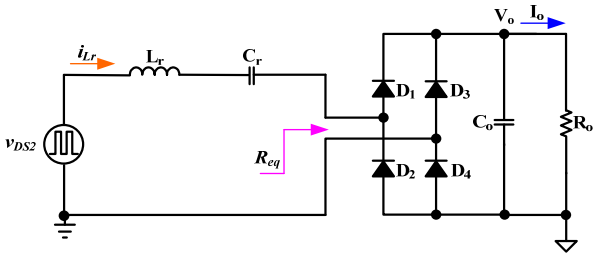

Figure 6. Equivalent circuit during the design of the series resonant tank.

Referring to Figure 6, the equivalent load resistance R_{eq} can be expressed as [24]

$$R_{eq} = \frac{8V_o}{\pi^2 I_o} = \frac{8}{\pi^2} R_o. \tag{6}$$

With a V_o of 60 V and an I_o of 0.3 A, the equivalent load resistance R_{eq} is given by

$$R_{eq} = \frac{8}{\pi^2}\left(\frac{60}{0.3}\right) = 162.1\ \Omega.$$

Referring to Figure 6, the series resonant tank is composed of a resonant inductor L_r in series connection with a resonant capacitor C_r; and the resonant frequency f_o can be expressed by

$$f_o = \frac{1}{2\pi\sqrt{L_r C_r}}. \tag{7}$$

The loaded quality factor Q_L is expressed by

$$Q_L = \frac{\sqrt{\frac{L_r}{C_r}}}{R_{eq}}. \tag{8}$$

In order to obtain ZVS for the two active switches, the switching frequency f_S is designed to be larger than the resonant frequency f_o so that the resonant tank resembles an inductive network [24].

Therefore, the relationship between switching frequency f_S and resonant frequency f_o is selected as

$$f_S = 4f_o. \tag{9}$$

Combining (7) and (8) with (9), the resonant capacitor C_r is given by

$$C_r = \frac{2}{\pi f_S R_{eq} Q_L}. \tag{10}$$

By selecting an f_S of 55 kHz and a Q_L of 0.9, the resonant capacitor C_r is computed as

$$C_r = \frac{2}{\pi \times 55k \times 162.1 \times 0.9} = 79.3\ \text{nF}.$$

In addition, C_r is selected to be 82 nF.

Combining (7) with (9), the resonant inductor L_r is given by

$$L_r = \frac{4}{\pi^2 {f_S}^2 C_r}. \tag{11}$$

With an f_S of 55 kHz and a C_r of 82 nF, the resonant inductor L_r is computed as

$$L_r = \frac{4}{\pi^2 \times (55k)^2 \times 82n} = 1.63 \text{ mH}.$$

4. Experimental Results

A prototype driver has been built and tested for supplying an 18 W-rated T8-type LED tube lamp (EVERLIGHT FBW/T8/857/U/4ft, ELECTRONICS Co., Ltd., New Taipei City, Taiwan), whose rated voltage and current are 60 V and 0.3 A, respectively. The components utilized in the LED tube lamp driver are shown in Table 1.

Table 1. Key components used in the presented led tube lamp driver.

Component	Value
Filter Inductor (L_f)	2 mH
Filter Capacitor (C_f)	0.68 μF/250 V
Diodes (D_{b1}, D_{b2})	MUR460
Power Switches (S_1, S_2)	IRF840
Coupled Inductors (L_{PFC1}, L_{PFC2})	1.34 mH
DC (direct current)-Linked Capacitors (C_{DC1}, C_{DC2})	100 μF/450 V
Resonant Inductor (L_r)	1.68 mH
Resonant Capacitor (C_r)	82 nF
Diodes (D_1, D_2, D_3, D_4)	MUR460
Output Capacitor (C_o)	200 μF/63 V

Figure 7 presents the measured inductor current i_{LPFC1}. The measured switch voltage v_{DS2} and inductor current i_{Lr} are shown in Figure 8, and the series resonant tank resembles an inductive load. The measured DC-bus voltage is shown in Figure 9, and the average value of V_{DC} is approximately 318 V. Figure 10a,b presents the measured voltages v_{DS1} and v_{DS2} and currents i_{DS1} and i_{DS2} of the power switches S_1 and S_2, respectively. ZVS is obviously achieved on the power switches; thus, the circuit efficiency is increased.

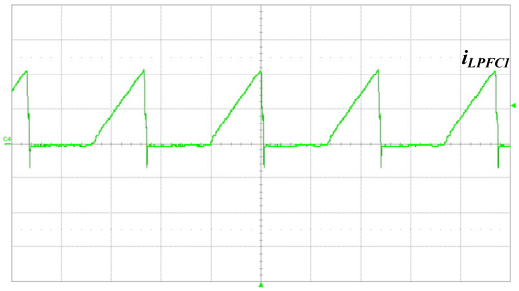

Figure 7. Measured inductor current i_{LPFC1} (0.5 A/div); time scale: 5 μs/div.

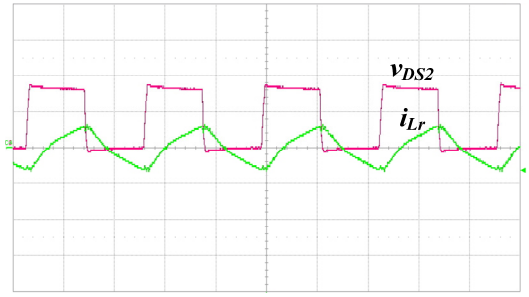

Figure 8. Measured voltage v_{DS2} (200 V/div) and inductor current i_{Lr} (1 A/div); time scale: 5 μs/div.

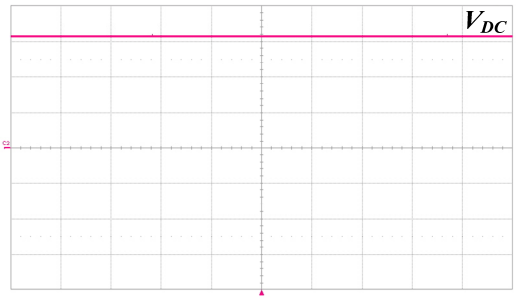

Figure 9. Measured DC (direct current)-bus voltage V_{DC} occurred on DC-linked capacitors (C_{DC1} and C_{DC2}) (100 V/div); time scale: 5 μs/div.

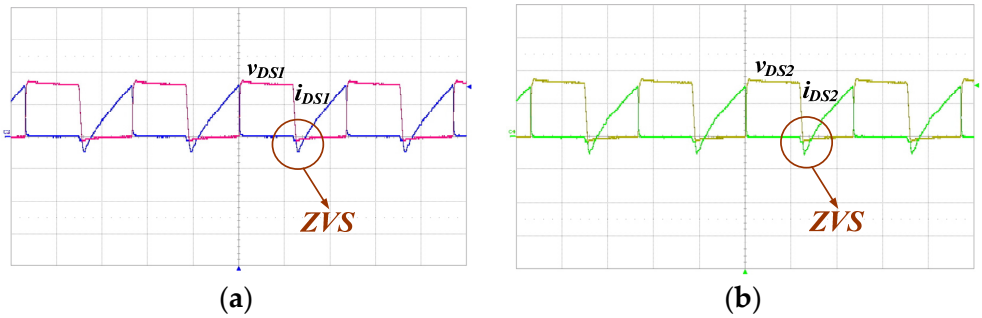

Figure 10. (**a**) Measured voltage v_{DS1} (200 V/div) and current i_{DS1} (1 A/div); time scale: 5 μs/div; (**b**) Measured voltage v_{DS2} (200 V/div) and current i_{DS2} (1 A/div); time scale: 5 μs/div.

Figure 11 shows the measured output voltage and current waveforms, and the average values of V_o and I_o are 60 V and 0.3 A, respectively. Table 2 presents the measured output voltage and current of the presented LED tube lamp driver under different input voltages. Figure 12 shows the calculated voltage and current ripple factors of the presented LED tube lamp driver under different input utility-line voltages. In addition, the output voltage (current) ripple factor is obtained by the peak-to-peak (pk–pk) level divided by the average value of output voltage (current). According to Figure 12, the highest and lowest measured output-voltage ripple factors are 7.2% and 6.26%; these occurred at a utility-line rms voltage of 120 V and 100 V, respectively. Moreover, the highest and lowest measured output-current ripple factors are 7.45% and 6.74%; these occurred at a utility-line rms voltage of 100 V and 120 V, respectively.

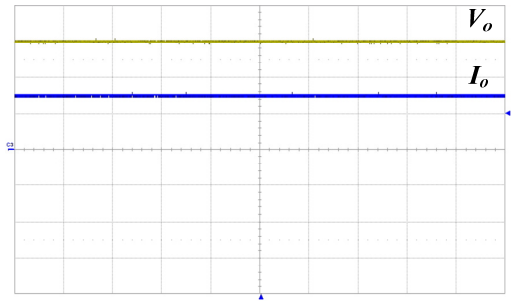

Figure 11. Measured output voltage V_o (20 V/div) and current I_o (0.2 A/div); time scale: 2 ms/div.

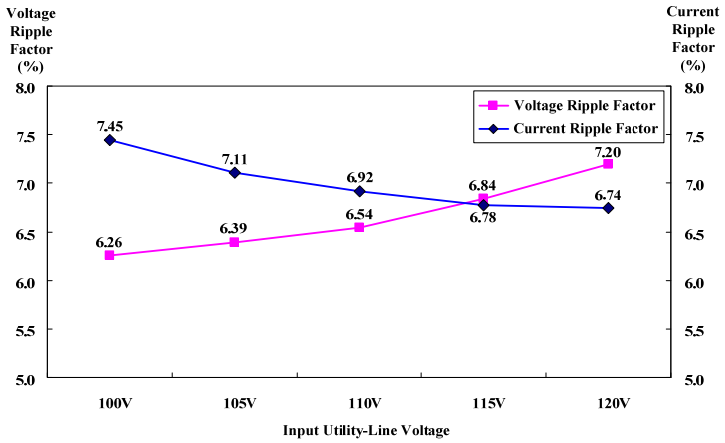

Figure 12. Calculated voltage and current ripple factors of the presented LED tube lamp driver under different input utility-line voltages.

Table 2. Measured output voltage and current of the presented led tube lamp driver under different input voltages.

Input Voltage / Parameters	100 V	105 V	110 V	115 V	120 V
Output Voltage (mean)	60.07 V	60.1 V	60.08 V	60.11 V	60.16 V
Output Voltage (pk–pk)	3.76 V	3.84 V	3.93 V	4.11 V	4.33 V
Output Current (mean)	0.321 A	0.311 A	0.308 A	0.304 A	0.301 A
Output Current (pk–pk)	23.9 mA	22.1 mA	21.3 mA	20.6 mA	20.3 mA

The measured input utility-line voltage and current are shown in Figure 13, and the input current is in phase with the input voltage. Figure 14 presents the measured input-current harmonics compared with the International Electrotechnical Commission (IEC) 61000-3-2 Class C standards under input utility-line voltages ranging from 100 V to 120 V; all measured current harmonics meet the requirements. Figure 15 shows the measured power factor (PF) and current THD at input utility-line voltages ranging from 100 V to 120 V. At a utility-line rms voltage of 110 V, the measured PF and current THD are 0.96 and 9.3%, respectively. The maximum PF is 0.97 occurred at a utility-line rms voltage of 120 V, and the minimum current THD is 6.9% occurred at a utility-line rms voltage of 100 V.

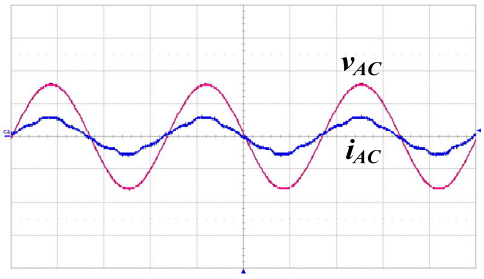

Figure 13. Measured input utility-line voltage v_{AC} (100 V/div) and current i_{AC} (0.5 A/div); time scale: 5 ms/div.

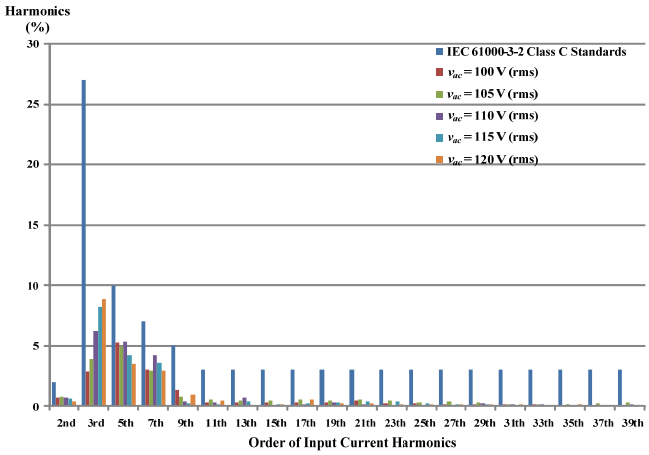

Figure 14. Measured input-current harmonics compared with the IEC 61000-3-2 Class C standards.

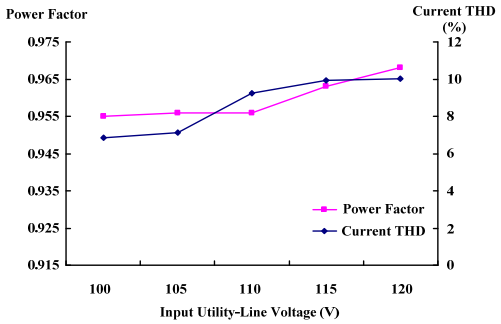

Figure 15. Measured power factor and current total-harmonic distortion (THD) of the presented LED tube lamp driver under different input utility-line voltages.

Figure 16 shows the measured efficiency of the presented LED tube lamp driver under input utility-line voltages from 100 V to 120 V. The highest and lowest measured efficiency levels are 94.16% and 91.24%; these occurred at utility-line rms voltages of 100 V and 120 V, respectively. In addition, the efficiency which drops with increased utility-line voltages is related to the voltage gain of the LC series-resonant tank. For providing rated output power (voltage/current), the voltage gain of the LC series-resonant tank will decrease when the utility-line voltages increase, resulting in increasing the switching frequency of the power switches. Thus, the switching losses of power switches and conduction losses of power diodes will increase resulting in lowering the circuit efficiency.

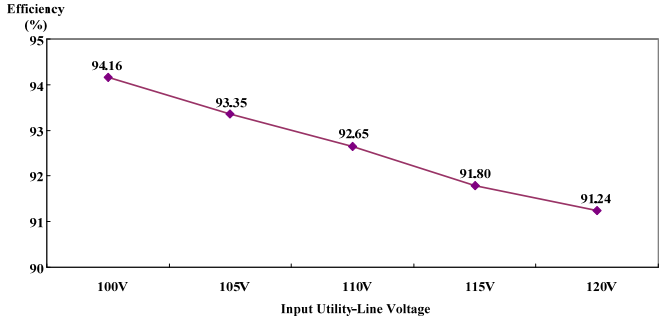

Figure 16. Measured efficiency of the presented LED tube lamp driver under different input utility-line voltages.

The comparisons between the existing T8-Type LED tube lamp drivers and the proposed one are shown in Table 3. A flyback-type AC-DC converter as an LED tube lamp driver is presented in [18], and a buck-type AC-DC converter as an LED tube lamp driver is presented in [19]. In addition, these existing LED tube lamp drivers ([18,19]) operate with universal input voltages while the proposed version operates with American utility-line voltages. Although the circuit components counts in the proposed driver are higher than these existing ones, this table illustrates that the proposed single-stage LED tube lamp driver has smaller input current THD and achieves soft-switching on the power switches to increase circuit efficiency over the two existing versions.

Table 3. Comparisons between the existing t8-type led tube lamp drivers and the proposed one.

Item	Existing LED (Direct Current) Tube Lamp Driver in [18]	Existing LED Tube Lamp Driver in [19]	Proposed LED Tube Lamp Driver
Circuit Topology	Flyback-type AC-DC (alternating current-direct current) Converter	Buck-type AC-DC Converter	Integration of a Dual Buck-Boost Converter with coupled inductors and a Half-Bridge Series Resonant Converter cascaded with a bridge rectifier
Input Utility-Line Voltages	90~264 V	90~264 V	100~120 V
Rated Output Power (Rated Output Voltage/Current)	19 W (42 V/0.45 A)	18.3 W (39 V/0.47 A)	18 W (60 V/0.3 A)
Required Power Switch	1 (Without Soft-Switching)	1 (Without Soft-Switching)	2 (With Soft-Switching)
Measured Maximum Power Factor	0.99 @ 110 V	0.96 @ 110 V	0.97 @ 120 V
Measured Minimum Input Current THD (total-harmonic distortion)	9% @ 180 V	21.54% @ 110 V	6.86% @ 100 V
Measured Maximum Efficiency	87.8% @ 180 V	88.56% @ 180 V	94.16% @ 100 V

5. Conclusions

This paper has presented and implemented a single-stage driver suitable for energy-saving indoor lighting applications, which integrates a dual buck-boost converter with coupled inductors and a half-bridge series resonant converter cascaded with a bridge rectifier, for supplying an LED tube lamp for T8/T10 fluorescent lamp replacements with power-factor corrections and soft switching. A prototype circuit has been successfully built and tested for supplying an 18 W-rated LED tube lamp with utility-line voltages ranging from 100 V to 120 V. The experimental results have demonstrated high efficiency (>91%), satisfying power-factor (>0.96), low current THD (<10%), and soft-switching of power switches in the presented LED tube lamp driver.

Acknowledgments: The authors would like to convey their appreciation for grant support from the Ministry of Science and Technology (MOST) of Taiwan under its grant with reference number MOST 103-2221-E-214-024.

Author Contributions: Chun-An Cheng conceived and designed the circuit. En-Chih Chang performed circuit simulations. Ching-Hsien Tseng and Tsung-Yuan Chung carried out the prototype driver, and measured as well as analyzed experimental results with the guidance from Chun-An Cheng. En-Chih Chang revised the manuscript for submission.

Conflicts of Interest: The authors declare no conflict of interest.

References

1. Bender, V.C.; Marchesan, T.B.; Alonso, J.M. Solid-state lighting: A concise review of the state of the art on LED and OLED modeling. *IEEE Ind. Electron. Mag.* **2015**, *9*, 6–16. [CrossRef]
2. Brañas, C.; Azcondo, F.J.; Alonso, J.M. Solid-state lighting: A system review. *IEEE Ind. Electron. Mag.* **2013**, *7*, 6–14. [CrossRef]

3. Liang, T.J.; Tseng, W.J.; Chen, J.F.; Wu, J.P. A novel line frequency multistage conduction LED driver with high power factor. *IEEE Trans. Power Electron.* **2015**, *30*, 5103–5115. [CrossRef]
4. Moo, C.S.; Chen, Y.J.; Yang, W.C. An efficient driver for dimmable LED lighting. *IEEE Trans. Power Electron.* **2012**, *27*, 4613–4618. [CrossRef]
5. Wang, Y.; Guan, Y.; Ren, K.; Xu, D. A single-stage LED driver based on BCM boost circuit and converter for street lighting system. *IEEE Trans. Ind. Electron.* **2015**, *62*, 5446–5457. [CrossRef]
6. Kwak, S.S. Pulse-driven LED circuit with transformer-based current balance technique. *Int. J. Electron.* **2014**, *101*, 1683–1693. [CrossRef]
7. Hsia, S.C.; Sheu, M.H.; Lai, S.Y. Chip implementation of high-efficient light-emitting diode dimming driver for high-power light-emitting diode lighting system. *IET Power Electron.* **2015**, *8*, 1043–1051. [CrossRef]
8. Choi, W.Y.; Yang, M.K. High-efficiency isolated SEPIC converter with reduced conduction losses for LED displays. *Int. J. Electron.* **2014**, *101*, 1495–1502. [CrossRef]
9. Chen, Y.S.; Liang, T.J.; Chen, K.H.; Juang, J.N. Study and implementation of high frequency pulse LED driver with self-oscillating circuit. In Proceedings of the IEEE International Symposium on Circuit and Systems (ISCAS), Rio de Janeiro, Brazil, 15–18 May 2011; pp. 498–501.
10. Wang, Y.; Guan, Y.; Zhang, X.; Xu, D. Single-stage LED driver with low bus voltage. *Eletron. Lett.* **2013**, *49*, 455–456. [CrossRef]
11. Hui, S.Y.R.; Li, S.N.; Tao, X.H.; Chen, W.; Ng, W.M. A novel passive off-line light-emitting diode (LED) driver with long lifetime. *IEEE Trans. Power Electron.* **2010**, *25*, 2665–2672. [CrossRef]
12. Qu, X.; Wong, S.C.; Tse, C.K. Resonance-assisted buck converter for offline driving of power LED replacement lamps. *IEEE Trans. Power Electron.* **2011**, *26*, 532–540.
13. Wang, Y.; Guan, Y.; Huang, J.; Wang, W.; Xu, D. A single-stage LED driver based on interleaved buck-boost circuit and LLC resonant converter. *IEEE J. Emerg. Sel. Top. Power Electron.* **2015**, *3*, 732–741. [CrossRef]
14. Chang, Y.N.; Kuo, C.M.; Cheng, H.L.; Lee, C.R. Design of dimmable LED lighting driving circuit for battery power source. In Proceedings of the 10th IEEE International Conference on Power Electronics and Drive Systems (PEDS), Kitakyushu, Japan, 22–25 April 2013; pp. 1168–1172.
15. Lin, C.C.; Yang, L.S.; Chang, E.C. Study of a DC-DC converter for solar LED street lighting. In Proceedings of the IEEE International Symposium on Next-Generation Electronics (ISNE), Kaohsiung, Taiwan, 25–26 February 2013; pp. 461–464.
16. Chen, N.; Chung, H.S.H. A driving technology for retrofit LED lamp for fluorescent lighting fixtures with electronic ballasts. *IEEE Trans. Power Electron.* **2011**, *26*, 588–601. [CrossRef]
17. Cheng, C.A.; Chang, E.C.; Tseng, C.S.; Chung, T.Y. A novel single-stage LED driver with coupled inductors and interleaved PFC. In Proceedings of the International Symposium on Computer, Consumer and Control, Taichung, Taiwan, 10–12 June 2014; pp. 1287–1290.
18. Texas Instruments. *19 W, Single-Stage AC/DC LED Driver for T8/T10 Fluorescent Lamp Replacement*; Texas Instruments: Dallas, TX, USA, 2011; pp. 1–21.
19. Fairchild Semiconductor. *User Guide for FEBFL7701 L34U018A Evaluation Board Universal Input 18.3 W LED Driver*; Fairchild Semiconductor: Sunnyvale, CA, USA, 2012; pp. 1–24.
20. Catalog of Lamps. China Electric MFG. Corporation. Available online: http://ebook.chinaelectric.com.tw/hosts/2/7/files/2712651479460151/book.php (accessed on 9 August2016).
21. Catalog of LED Lamps. Everlight Electronics Co., Ltd. Available online: http://www.everlightlighting.com/file/image/files/ELL_2015_Catalogue_dealer.pdf (accessed on 18 May 2015).
22. Cheng, C.A.; Cheng, H.L.; Chung, T.Y. A novel single-stage high-power-factor LED street-lighting driver with coupled inductors. *IEEE Trans. Ind. Appl.* **2014**, *50*, 3037–3045. [CrossRef]
23. Steigerwald, R.L. A comparison of half-bridge resonant converter topology. *IEEE Trans. Power Electron.* **1988**, *3*, 174–182. [CrossRef]
24. Kazimierczuk, M.K.; Czarkowski, D. *Resonant Power Converters*; Wiley: New York, NY, USA, 1995.